Opt Quant Electron (2017) 49:159
DOI 10.1007/s11082-017-0998-3

Mechanism investigation of a narrow-band super absorber using an asymmetric Fabry–Perot cavity

Qiang Li[1,2] · Jinsong Gao[1,2] · Haigui Yang[1] · Xiaoyi Wang[1] · Hai Liu[1] · Zizheng Li[1]

Received: 13 July 2016 / Accepted: 17 March 2017 / Published online: 22 March 2017

Abstract We propose a metal–insulator-metal super absorber based on an asymmetric Fabry–Perot cavity, by which a perfect narrow-band absorption can be achieved. In this structure, two silver layers form a cavity spaced by a lossless silicon oxide layer. The absorption of the absorber can reach about 98% and its absorption peak can be tuned by altering the thickness of the middle SiO_2 layer. We further present a deep comprehension on the physics mechanism of such high absorption. This super absorber can be easily fabricated by mature thin film technology, which make it an appropriate candidate for photodetectors, sensing, and spectroscopy.

Keywords Super absorber · Thin film · Metal–insulator-metal structure · Fabry–Perot cavity

1 Introduction

Super electromagnetic absorber attracts much attention due to its important application in solar cell, photo detection, sensing, and thermal emitting (Claire et al. 2012; Stephen and Wei 2012; Yen et al. 2012; Hamidreza et al. 2014; Byoungchoo et al. 2014; Thomas et al. 2016; Costantini et al. 2015). In recent years, plasmonic structures provide an unprecedented way to control the interaction between light and matter at nanoscale in order to achieve reflection, transmission, and absorption. These nanostructures such as nanowire, nanohole array, and nanodisk could excite localized surface plasmon resonances (LSPR) resulting in the enhancement of absorption (Lin et al. 2010; Qiang et al. 2016; Chuan et al.

✉ Qiang Li
liqiang113@mails.ucas.ac.cn

[1] Key Laboratory of Optical System Advanced Manufacturing Technology, Changchun Institute of Optics, Fine Mechanics and Physics, Chinese Academy of Sciences, Changchun 130033, China

[2] University of the Chinese Academy of Sciences, Beijing 100039, China

2014; Xiang et al. 2016). Absorbers based on plasmonic structures exhibit an ultra-high absorption by engineering the geometry, size, and periodicity of the structures. However, these nanostructures usually involve costly precise manufacturing and nano fabrication process steps such as electron beam lithography (EBL) and focused ion beam (FIB) which turn out to be a challenge for the application in large area of these patterned absorber.

Planar, unpatterned and multilayer optical coatings consisted of one or more films of metallic or dielectric materials are widely used as Fabry–Perot cavity and Bragg-reflector mirror (Jian et al. 2016; Renato et al. 2016; Yan et al. 1998; Minkyu et al. 2015). Early in 1952, a three-layer structure consisted of a metallic ground plane, a lossless dielectric middle layer, and a thin glossy top layer, was designed as super absorber for the military radar waves (Salisbury 1952). Most recently, Mikhail et al. proposed a simple design for perfect absorption based on ultrathin and lossy layer structure (Germanium ultrathin film and Gold reflection mirror), which confirms that continuous, unpatterned, and ultra-thin film also could be a candidate for super absorber and inspires the interest in thin film optical device (Mikhail et al. 2013).

In this work, we propose a three-layer thin film structure (metal–insulator-metal, MIM) which could exhibit a near unity absorption in a narrow band and give a deep comprehension on the reason of ultra-high absorption. Compared to plasmonic structures, our MIM absorber based on Fabry–Perot (FP) cavity not only could be easily fabricated by mature thin film technology instead of costly nano fabrication techniques, but its optical spectrum is controlled conveniently by the thickness of the layers rather than the size of the nanostructures. Therefore, the proposed large-area, simple and low-cost absorber is promising for photodetectors, photovoltaics, sensing, and spectroscopy.

2 Experiment design and fabrication

The proposed absorber was fabricated on the K9 glass substrate. Before the deposition of thin films, the K9 glasses were cleaned using ultrasonic cleaning in acetone solution for 10 min. The Ag layer was deposited by DC reactive magnetron sputtering at a rate of 4.28 As^{-1} with 150 w power, 1.0 Pa pressure. While the SiO_2 layer was deposited by the method of RF reactive magnetron sputtering at a rate of 0.63 As^{-1} with 80 w power, 1.0 Pa pressure. The reflection spectrums (R) of the fabricated samples at normal incidence were measured by using a spectrometer (PerkinElmer Lambda-1050). And then the experimental absorption (A) was calculated by the equation A = 1-R because the bottom Ag layer is thick enough to completely inhibit the transmission.

3 Experimental results and discussion

Our representative geometry is schematically shown in Fig. 1a, which consists of three planar thin films. We choose K9 glass as substrate and design the geometrical thickness $t = 30$ nm, $h = 100$ nm for the top Ag thin film and bottom Ag reflection mirror respectively. In this structure, Ag is chosen for its low material absorption and highest reflection in the entire visible wavelength range. The thickness of bottom Ag layer is set to be 100 nm which could assure no light pass through. The top Ag layer is optimized to 30 nm for the best absorption, which will be discussed in the following section. SiO_2 is

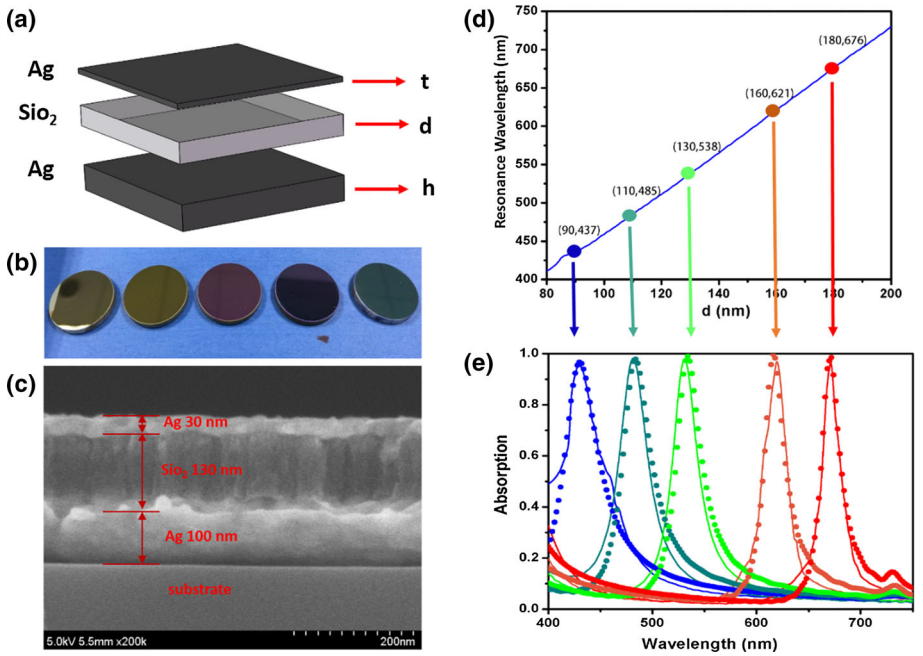

Fig. 1 **a** Schematic diagram of the MIM structure absorber. The thickness of the layers are t, d, and h respectively. **b** The fabricated samples with five different thickness d = 90 nm, 110 nm, 130 nm, 160 nm and 180 nm from left to right (t = 30 nm, h = 100 nm). **c** SEM image of the prepared structure showing the Ag and SiO_2 layers. **d** The relationship of resonance wavelength and the thickness d calculated by the Transfer Matrix Method (TMM). **e** The *five colorful solid lines* represent the measured absorption spectrums when the thickness of the SiO_2 are d = 90, 110, 130, 160 and 180 nm, respectively. The *five colorful solid dots* express the simulated results by Finite-Difference Time-Domain (FDTD) algorithm. (Color figure online)

selected for its high transparency and no loss optical properties over the visible wavelength range.

The three-layer MIM structure is an asymmetric Fabry–Perot cavity. The top and bottom Ag layers can form a resonator cavity. The middle SiO_2 is the spacing layer whose thickness determines the resonance wavelength. We first use the Transfer Matrix Method (TMM) (Yeh 2005) to calculate the absorption spectrums of this three-layer MIM structure with the thickness of SiO_2 from 80 to 200 nm by a 1 nm interval and plot the resonance wavelength as a function of the thickness d in Fig. 1d. The optical constant of Ag and SiO_2 used in calculation are extracted from the data of Palik (Palik 1991). As the blue line in Fig. 1d shows, the relationship of resonance wavelength and the thickness d is linear variation approximately. The linear dependence of the resonance upon d suggests that the underlying mechanism may be ascribed to the FP resonance. We choose five different thickness of d = 90, 110, 130, 160, 180 nm and deposit Ag and SiO_2 layers alternately on the glass substrate via magnetron sputtering in a vacuum chamber. The fabricated samples present five different vivid colors from left to right corresponding to the five thickness as Fig. 1b shows. The cross-section SEM image of the prepared structure showing the Ag and SiO_2 layers clearly in Fig. 1c. Their experimental absorption spectrums (the solid lines) are shown in Fig. 1e which are agree perfectly with the simulation results (the solid dots) by the Finite Difference Time Domain (FDTD) algorithm. As the measured results show, the

absorption of this MIM structure with various d (90, 110, 130, 160 and 180 nm) can reach about 98% at different resonance wavelengths. Their full width at half maximum (FWHM) is from 20 to 56 nm, leading to the highest quality factor (Q) of 33.6 ($Q = \lambda/\Delta\lambda$). The experiment results contracting with simulation at resonance wavelengths are showed in Table 1 for details.

The experiment measured and numerical simulation results indicate that our three-layer MIM structure based on FP cavity could achieve a near unity absorption at resonance wavelength. In order to understand the reason of such high absorption, we discuss the effect of different top Ag layer thickness t on absorption. We first use FDTD algorithm to simulate the reflection (R), transmittance (T) of a single Ag layer with a thickness from 0 to 80 nm by an interval of 1 nm and calculate its absorption by $A = 1 - R - T$, as the Fig. 2a shown. The absorption of single Ag layer mainly concentrates in high frequency region which is determined by the material property of Ag and the resonant behavior is not observed. In contrast to the non-resonant absorption of single Ag layer, the MIM structure behaves resonant absorption as the simulation results shown in Fig. 2b where we fix the thickness of middle SiO_2 layer to be 130 nm. When the thickness of top Ag layer is 0 nm, the MIM structure turns to be an Ag reflection mirror coated by a SiO_2 layer. In this case the reflection is ultrahigh which leads to an almost zero absorption. Increasing the Ag thickness, we can observe a resonant absorption peak due to the FP cavity. For 30 nm-thick top Ag layer the resonance wavelength is approximately 538 nm, which is in accord with the green line in Fig. 1d, e. Consequently, the super absorber we proposed is coated with 30 nm thick top Ag layer for the perfect absorption.

In order to clarify the physics mechanism of absorption, we simulate the distributions of electric field (|E|) at resonance (538) and non-resonance (650) wavelength respectively for MIM structure with 130 nm SiO_2 and 30 nm top Ag layers. As the FDTD simulation result shown in Fig. 3a, at non-resonance wavelength of 650 nm, the electric field (E-field) is concentrated in the air above the top Ag layer and there is little E-field enhancement in the middle SiO_2 layer because of the ultrahigh reflection. However, for resonance wavelength of 538 nm, we can observe from Fig. 3b that the E-field is highly confined between top and bottom Ag layer leading to a four-time enhancement in the middle SiO_2 layer, which means the two Ag layers form a resonance cavity. The incident light with resonance wavelength determined by the thickness of SiO_2 layer can be reflected constantly by the both Ag layers and loss some power in Ag layers every time reflected until all the power is consumed. Obviously, our MIM structure is different from the traditional FP cavity which relies on interference theory as the description in these references (Jian et al. 2016; Renato

Table 1 The experiment and simulation results at resonance wavelengths for five different thickness of d = 90, 110, 130, 160 and 180 nm

d (mm)	Simulation results		Measured results		
	Resonance wavelength (nm)	Max absorption	Resonance wavelength (nm)	Max absorption	FWHM (nm)
90	437	0.9669	440	0.9828	56
110	485	0.9787	482	0.9845	32
130	538	0.9889	530	0.9797	28
160	621	0.9966	620	0.9825	24
180	676	0.9964	672	0.9817	20

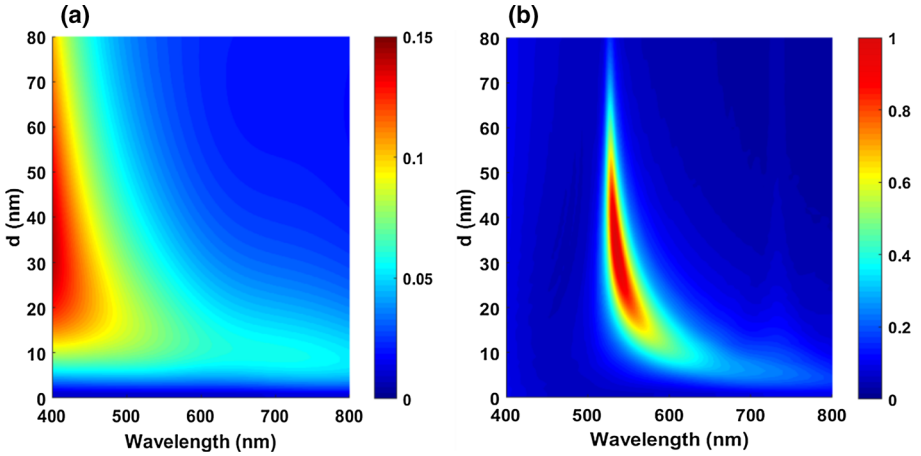

Fig. 2 Absorption simulated by FDTD algorithm. **a** The absorption as a function of wavelength of a single Ag layer with different thickness from 0 to 80 nm. **b** The absorption as a function of wavelength of the MIM structure with top Ag thickness from 0 to 80 nm

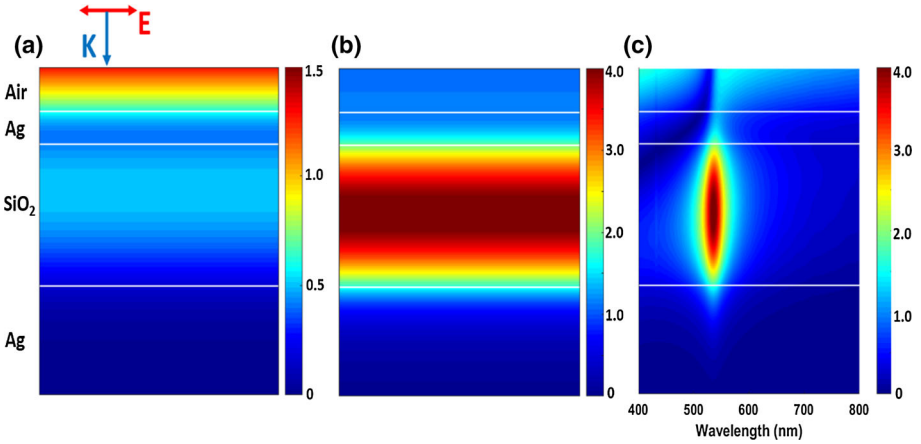

Fig. 3 The three layers of MIM absorber consists of 100 nm bottom Ag layer, 130 nm middle SiO_2 layer and 30 nm top Ag layer. **a**, **b** Simulated electric field amplitude distributions at non-resonance wavelength of 650 nm and resonance wavelength of 538 nm respectively. **c** Simulated electric field amplitude distributions as a function of wavelength in the visible region

et al. 2016; Yan et al. 1998). In traditional Fabry–Perot cavity, the beams reflected by the two mirrors could form constructive and destructive interference according to the phase shift when the light pass through the middle insulator layer, while our MIM absorber can select the resonance wavelength relying on the FP cavity effect but importantly the light selected is consumed in both Ag layers, which is the main difference from traditional FP cavity. We also simulate the distributions of electric field (|E|) at all visible wavelengths shown in Fig. 3c. As we can see, for 130 nm thick SiO_2 layer, the E-field is greatly enhanced at the resonance wavelength 538 nm according with Fig. 3b, and moreover the E-field enhancement band is narrow agreed with the narrow absorption in Fig. 1e. The simulation results indicate that the three-layer MIM structure implement its function by FP

cavity and the absorption has some relations with the E-field enhancement which we will discuss later. Although we only discussed the situation for a typical MIM structure with 130 nm middle SiO_2 layer, similar results could be observed for other case with different thickness of SiO_2 layer.

For better understanding the relation of absorption and the E-field enhancement, we use FDTD algorithm to calculate the absorption of three layers respectively at the resonance wavelength of 538 nm for the MIM structure with 130 nm thickness middle SiO_2 and 30 nm top Ag layer. We set power monitors from bottom Ag layer to top Ag layer by an interval of 1 nm to record the power intensity when incident light passes through them. The different values between two adjacent monitors represent the absorption by the layer between two monitors. As the simulation result shows in Fig. 4a, the incident light is absorbed by both two Ag layers and the power absorption is mainly concentrated in the top Ag layer. We also calculate the absorption in the top and bottom Ag layers are about 60.75 and 37.18% respectively. The remaining 2% is reflected back and not absorbed by the absorber.

In addition, the absorption distribution in the MIM absorber can be directly calculated numerically by using the local ohmic loss for non-magnetic materials (Vivian et al. 2008; Wei and Jason 2014):

$$Q(r,w) = \frac{1}{2} \times w \times \mathrm{Im}(\varepsilon) \times E^2(r,w) \tag{1}$$

where w is the angular frequency, $Im(\varepsilon)$ is the imaginary part of the dielectric permittivity and E (r, w) is the local electric field. Here the electric field amplitude distributions we use are the simulation results from Fig. 3a, b and the square of E-field amplitude distributed in the space at the resonance wavelength of 538 nm is plotted in Fig. 4b. The total absorption within the three-layer MIM stack calculated by using the Eq. (1) is plotted in Fig. 4c. As we can see, the blue line indicates the ohmic loss at the resonance wavelength of 538 nm is much larger than the red line at non-resonance wavelength of 630 nm which is due to the different E-field amplitude distributions as Fig. 4b shows. The stronger the E-field in

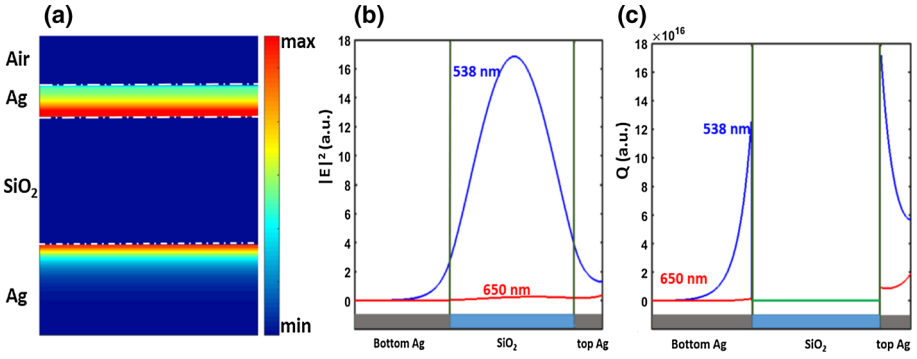

Fig. 4 The three layers of MIM absorber consists of 100 nm bottom Ag layer, 130 nm middle SiO_2 layer and 30 nm top Ag layer. **a** Simulated absorption in the three layers at the resonance wavelength of 538 nm. **b** *Square* of the simulated electric field amplitude. *Blue line* is for resonance wavelength of 538 nm and *Red line* is for non-resonance wavelength of 650 nm. **c** The total absorption within the three-layer MIM stack calculated by using the formula (1). The *blue and red line* is for the wavelength of 538 and 650 nm respectively and the *green line* indicates that the absorption is zero in the middle SiO_2 layer for both 538 and 650 nm. (Color figure online)

metal, the more power it can consume. Therefore, we prove that the dominant absorption occurs in both metal layers especially in the top Ag layer in theory.

4 Conclusion

In conclusion, the three-layer MIM absorber we proposed based on Fabry–Perot cavity could reach about 98% absorption with a narrow bandwidth 20–56 nm by both experiment and simulation. We clarified the function of each layer in the MIM structure and presented a deep understanding of the physics mechanism of super absorption. We used simulation and theory to explain that the absorption in metal is determined by the E-field distributions. It exhibits a higher absorption where the E-field is stronger due to cavity effect. The ultrahigh absorption in our absorber does not rely on any plasmonic effect and it can be deposited by using single magnetron sputtering. This makes it an appropriate candidate for photodetectors, photovoltaics, sensing, and spectroscopy.

Acknowledgements This work was supported by the National Natural Science Foundation of China (Nos. U1435210, 61306125, 61675199 and 11604329), the Science and Technology Innovation Project (Y3CX1SS143) of CIOMP, the Science and Technology Innovation Project of Jilin Province (Nos. 20130522147JH and 20140101176JC).

References

Byoungchoo, P., Soo, H.Y., Chan, Y.C., Young, C.K., Jung, C.S., Hong, G.J., Yoon, H.H., Inchan, H., Ku, Y.B., Young, I.L., Han, S.U., Guang, S.C., Eun, H.C.: Surface plasmon excitation in semitransparent inverted polymer photovoltaic devices and their applications as label-free optical sensors. Light Sci. Appl. **3**, e222 (2014)

Chuan, F.G., Tianyi, S., Feng, C., Qian, L., Zhifeng, R.: Metallic nanostructures for light trapping inenergy-harvesting devices. Light Sci. Appl. **3**, e161 (2014)

Claire, M.W., Xianliang, L., Willie, J.P.: Metamaterial electromagnetic wave absorbers. Adv. Mater. **24**, 98–120 (2012)

Costantini, D., Lefebvre, A., Coutrot, A.L., Moldovan-Doyen, I., Hugonin, J.P., Boutami, S., Marquier, F., Benisty, H., Greffet, J.J.: Plasmonic metasurface for directional and frequency-selective thermal emission. Phys. Rev. A **4**, 014023 (2015)

Hamidreza, C., David, S., Mark, L.B.: Hot-electron photodetection with a plasmonic nanostripe antenna. Nano Lett. **14**, 1374–1380 (2014)

Jian, W., Wei, B.L., Xiao, B.L., Ji, L.L.: Terahertz wavefront control based on graphene manipulated Fabry–Pérot cavities. IEEE Photon. Technol. Lett. **28**, 971–974 (2016)

Lin, Y.C., Peng, Y.F., Alok, P.V., Justin, S.W., Zong, F.Y., Wen, S.C., Jon, A.S., Shanhui, F., Mark, L.B.: Semiconductor nanowire optical antenna solar absorbers. Nano Lett. **10**, 439–445 (2010)

Mikhail, A.K., Romain, B., Patrice, G., Federico, C.: Nanometre optical coatings based on strong interference effects in highly absorbing media. Nat. Mater. **12**, 20–24 (2013)

Minkyu, C., JungHun, S., Jaeseong, L., Deyin, Z., Hongyi, M., Xin, Y., Munho, K., Xudong, W., Weidong, Z., Zhenqiang, M.: Ultra-thin distributed bragg reflectors via stacked single-crystal silicon nanomembranes. Appl. Phys. Lett. **106**, 181107 (2015)

Palik, E.D.: Handbook of Optical Constants in Solids. Academic Press, San Diego (1991)

Qiang, L., Zizheng, L., Haigui, Y., Hai, L., Xiaoyi, W., Jinsong, G., Jingli, Z.: Novel aluminum plasmonic absorber enhanced by extraordinary optical transmission. Opt. Express **24**, 25885–25893 (2016)

Renato, O., Alberto, T., Pierluigi, D.: Bimodal resonance phenomena—part I: generalized Fabry-Pérot interferometers. IEEE J. Quantum Electron. **52**, 6100508 (2016)

Salisbury, W.W.W.: Absorbent body for electromagnetic waves. Patent US 2599944 (1952)

Stephen, Y.C., Wei, D.: Ultrathin, high-efficiency, broad-band, omniacceptance, organic solar cells enhanced by plasmonic cavity with subwavelength hole array. Opt. Express **21**, A60–A76 (2012)

Thomas, A., Raz, A., Ron, N., Kyriacos, K., Vojte, K., Aleksey, R., Phil, C., David, J.W.: Photonic gas sensors exploiting directly the optical properties of hybrid carbon nanotube localized surface plasmon structures. Light Sci Appl. **5**, e16036 (2016)

Vivian, E.F., Luke, A.S., Domenico, P., Harry, A.: Plasmonic nanostructure design for efficient light coupling into solar cells. Nano Lett. **8**, 4391–4397 (2008)

Wei, L., Jason, V.: Metamaterial perfect absorber based hot electron photodetection. Nano Lett. **14**, 3510–3514 (2014)

Xiang, C.M., Ying, D., Lin, Y., Bai, B.H.: Energy transfer in plasmonic photocatalytic composites. Light Sci. Appl. **5**, e16017 (2016)

Yan, R.H., Simes, R.J., Coldren, L.A.: Electro absorptive Fabry–Perot reflection modulators with asymmetric mirrors. IEEE Photon. Technol. Lett. **9**, 1041–1135 (1998)

Yeh, P.: Optical Waves in Layered Media. Wiley, New York City (2005)

Yen, H.S., Yuan, F.K., Shi, L.C., Qian, Y.Y.: Surface plasmon resonance of layer-by-layer gold nanoparticles induced photoelectric current in environmentally-friendly plasmon-sensitized solar cell. Light Sci. Appl. **1**, e14 (2012)